CrossLinking of Biobased Monofunctional Furan Epoxy Monomer by Two Steps Process, UV Irradiation and Thermal Treatment

RESEARCH ARTICLE

Macromolecular Chemistry and Physics
www.mcp-journal.de

Cross-Linking of Biobased Monofunctional Furan Epoxy Monomer by Two Steps Process, UV Irradiation and Thermal Treatment

*Lorenzo Pezzana, Giuseppe Melilli, Nathanael Guigo, Nicolas Sbirrazzuoli, and Marco Sangermano**

Among the new generation of green polymers, furan monomers are occupying a strategic role to produce both innovative biobased thermoplastic and thermoset. Herein, furfuryl glycidyl ether (FGE) is used as monomer to design two steps cured coating. Linear polymer chains are first produced by means of cationic UV technique. The UV reactivity of FGE is assessed by real-time Fourier Transform Infrared Spectroscopy (FTIR). Then, a thermal treatment is carried out to crosslink the UV-irradiated linear chains. The formation of cross-links is proven by means of different techniques. ATR-FTIR shows the development of new chemical bonds by the appearance of new bands. Differential scanning calorimetry analysis confirms the cross-link reaction by the presence of exothermic peaks and the dynamic mechanical thermal analysis reveals an increase of the T_g as direct consequence of cross-links formation. Moreover, the %gel analysis confirms the formation of highly insoluble fraction after the cross-linking.

1. Introduction

The development and implementation of biobased polymers has rapidly increased in recent years driven by environmental concerns. Green resources from terrestrial plant biomass such as agricultural residues or forestry wastes has becoming crucial to develop new monomers. The purpose of the new researches is to substitute petroleum monomers in order to decrease the pollution, to reduce the exploitation of fossil fuel and to limit the waste disposal.[1,2] Furan-based monomers are currently exploited in many applications due to the large availability of biomass, the relatively low cost of the resource and the worldwide availability.

Among others, monosaccharides contained in hemicellulose—a key component of vegetable biomass with lignin and cellulose[3]—can lead upon dehydration to furanic building blocks. Pentose and hexose are the main units to produce different furan-based monomers. Specifically, furfuryl alcohol (FA) is one of the monomers derived from furfural and it represents the highest percentage among all the several available derivatives.[4] Furfuryl alcohol has been used to produce fuels, fine chemicals and biobased polymers.[5] FA was used in polyurethane and polyester foams; it can be used as reinforcement and it can be also exploited in coating applications.[6–8] The resins derived from FA are capable to substitute phenolic resin and FA is also a key component in developing epoxy resin.[9,10]

The outstanding feature of FA is its intrinsic possibility to have self-condensation reaction on furfuryl units initiated by acids. These initial condensation reactions are followed by hardening giving the possibility to tailor the properties of the final polyfurfuryl alcohol (PFA) resin.[11,12] The darkening and cross-linking mechanism in PFA was initially explained by Choura et al.[13] and confirmed by several further studies.[14,15]

Considering the actual level of concern toward the utilization of green processes in combination with green resources, the UV-curing is having a great interest. Indeed, due to the need of limiting energy consumption and pushing the industry to sustainability, UV-curing is representing a different way to produce thermosets with respect to traditional thermal curing. It has several advantages such as high curing speed and lack of volatile organic compounds emissions.[16–20] Crivello was one of the first experts on cationic UV-curing in the late 20th; he discovered several classes of specific photoinitiator for cationic process, such as the diaryliodonium salt or the dialkylphenacylsulfonium salts. These molecules, through photolysis, can generate strong acidic species able to initiate the cationic chain-growth polymerization.[21,22] Several biobased monomers have been used in UV-curing exploiting both radical and cationic mechanism. Lignin derivatives such as ferulic acid, vanillin but also rosins derivatives has been employed in UV process exploiting the radical curing

L. Pezzana, M. Sangermano
Dipartimento Scienza e Tecnologia dei Materiali
Politecnico di Torino
Corso Duca degli Abruzzi 24, Torino 10100, Italy
E-mail: marco.sangermano@polito.it
G. Melilli, N. Guigo, N. Sbirrazzuoli
Institut de Chimie de Nice Université Côte d'Azur CNRS
UMR 7272, Nice 06108, France

DOI: 10.1002/macp.202200012

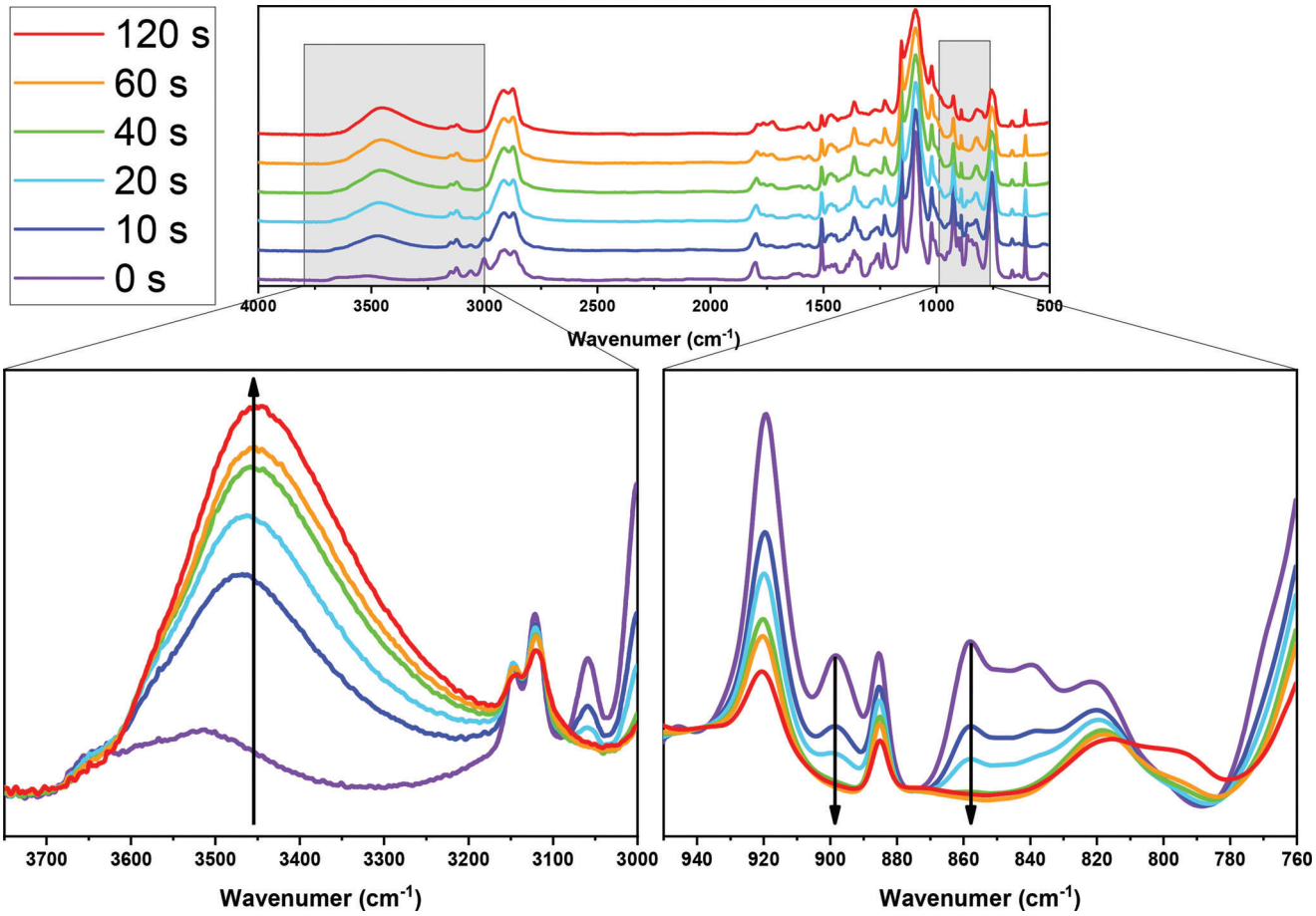

Figure 1. The real-time spectra for the cationic UV-curing of **FGE** in presence of 2 phr of photoinitiator. On the left side the increasing of the peak for the stretching of the OH group is reported while on the right there is the decrease through the time of the epoxy peaks situated around 900 and 860 cm^{-1}. The intensity of the lamp was set as 130 mW cm^{-2} and the film was coated on silicon wafer with a thickness of 12 μm.

while vegetable oils and terpenes has been used for cationic UV-curing.[23,24] Considering specifically the epoxy derivatives, Crivello and Narayan.[25] investigated the behavior of epoxides oils in photopolymerization. Noè et al.[26–28] deeply explored the cationic UV-curing of biobased epoxy monomers derived from vegetable oils. They used different types of oil from cardanol to soybean investigating several features of the formed thermosets. Recently furan-based monomers have been used in UV-curing to develop coatings and adhesives.[29,30]

Here we report the cross-linking of a synthetized furan monofunctional epoxy monomer (FGE) with two steps process: UV-irradiation and thermal treatment. The epoxy monomer was synthetized starting from furfuryl alcohol by one step reaction. Then the new curing process was developed to achieve thermoset from a monofunctional monomer. The novelty is related to the possibility to achieve the formation of a thermoset exploiting only a monofunctional monomer. The first stage of the UV-induced polymerization allowed to form linear polymer chains due to the reaction of the FGE in presence of cationic photoinitiator while the second step induced a cross-linking reaction among the different polymer chains. The investigation of the UV-irradiation was followed by Fourier transform infrared spectroscopy (FTIR) analysis and differential scanning calorimetry (DSC) measurements. The thermo mechanical behavior of the polymer network was studied by means of dynamic mechanical thermal analysis (DMTA).

2. Results and Discussion

Biobased furfuryl alcohol was functionalized with epoxy functionalities to exploit in cationic UV-light process. The epoxidation of furfuryl alcohol is reported in the experimental part and the efficiency reached a yield of 78%. The synthesis gave **FGE** as pure product as demonstrated by Nuclear Magnetic Resonance (NMR) analysis without requiring important purification step (Figures S1 and S2, Supporting Information). The advantage of this method includes a limited amount of solvents and relatively short time to reach high conversion of **FGE**. Successively, the biobased monofunctional epoxy monomer was investigated in cationic photopolymerization process. The photopolymerization was followed by real-time FTIR.

As it can be noticed in **Figure 1**, the bands attributed to the epoxy ring at 900 and 860 cm^{-1} decreased through the irradiation time reaching a complete conversion upon 2 min of irradiation, while it is possible to observe the increase of the stretching peak related to OH groups due to the ring-opening of the epoxy rings.

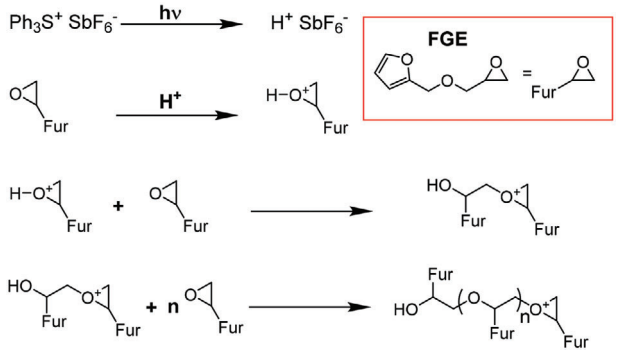

Scheme 1. Linear polymeric chain derived from UV-irradiation of epoxy monofunctional **FGE** in the presence of the cationic photoinitiator.

The conversion curve as a function of irradiation time, evaluated by the integration of the peak area at 860 cm^{-1} is reported in Figure S3 in the Supporting Information. The photopolymerization of monofunctional monomer gave rise to linear chains,[20] and in **Scheme 1** it is reported a possible schematic structure. The mass spectrometry analysis was carried out to demonstrate the formation of the linear polymer chains investigating their molecular weight. The result, reported in Figure S4 (Supporting Information), highlights the formation of polymer with and average molecular weight of 437 g mol^{-1}. Considering the molecular weight of the monomer unit (154 g mol^{-1}), it is possible to affirm that the average of units present in the chains are 2.8. Thus, the outcome of the UV-irradiation is a predominant formation of chains with three monomer units. The result is in accordance with previous study on formation of linear polymer by cationic UV-process.[31]

The cross-linked polymer network was achieved by a thermal treatment on the UV-irradiated formulation. The presence of the acid, previously formed by the photolysis of the photoinitiator, created the condition for the thermally induced cross-linking process.

Indeed, the furfuryl alcohol (FA) undergoes similar behavior in presence of acid and it is well demonstrated in literature the cross-linking of different furan rings of PFA networks.[14,15] Thus, considering the linear structure originated from the UV-irradiation of the monofunctional epoxy monomer and the presence of the acid catalyst, the cross-link process could happen leading to formation of a thermoset. The further characterizations were done to verify the change in the structure and to analyze the improvement of the properties caused by the formation of cross-links between the polymeric chains.

After the UV-irradiation we observed the appearance of four distinct peaks at 1762, 1719, 1562, and 1458 cm^{-1} (**Figure 2**). These peaks might be associated with a two-steps mechanism towards the formation of alpha/beta-angelica lactone (**Scheme 2**, Mechanism 1). As reported by Falco et al.,[32] the ring opening of furfuryl alcohol undergoes different chemical reactions which leads to the formation of levulinic acid (LA). The super-acidic condition could further catalyze the ring closure of LA yielding to alpha-angelica lactone.[33,34] This result is confirmed by the presence of the bands 1762 cm^{-1} (C═O stretching of the ester lactone), 1562, 1458 cm^{-1} carboxylate (O–C–O) stretching modes.[34] The band at 1719 cm^{-1} is assigned with the carbonyl of saturated ketones probably due to a residual LA in the system. The ring opening of the furan is also confirmed by the reduced intensity of the bands at 1503, 1149, 920, and 884 cm^{-1}.[14,15]

Nonisothermal real-time FTIR has been carried out to further demonstrate the structure variation induced upon heating. The resulted spectra in function of the temperature are reported in **Figure 3**. Between 1550 and 1750 cm^{-1} shoulders and new bands appears consequently to the ring opening reactions starting from 110 °C. In particular, the shoulder **3** at 1675 cm^{-1} is assigned to conjugated carbonyls also observed in ring opening of PFA.[14,35] The new band **5** is characteristic of C═C stretching vicinal to α, β unsaturated C═O.[14] Unlike the ring opening under UV light, the Mechanism 2 (Scheme 2) seemed to be favored over Mechanism 1 by the increase of the temperature. This led to formation of the structure **V**.

The occurrence of Diels–Alder cycloadditions is confirmed by the presence of two signals: the saturated C═O stretching vibration **2**, and C═C stretching **4**. The Diels–Alder reaction could happen between the furan ring (**IV**, diene) and the double bond belonging to the structure (**V**) (dienophile). Nevertheless, the Diels–Alder cycloaddition could also take place between the furan and the lactone (structure **III**) previously formed. Similar reactions have been reported in presence of cyclopentadiene.[36] In fact, by increasing the temperature the characteristic peaks of the lactone **1**, **6**, and **8** decrease.

Due to ring opening reaction and Diels–Alder reaction with the temperature all the main furan characteristic bands (**7**, **9**, **10**, **11**, **12**, **13**, **14**, and **15**) are strongly reduced during the nonisothermal curing.

The proper thermal postcuring process conditions were established by DSC analysis. In **Figure 4**a the isothermal curing heat flow curves as a function of time are reported for the **FGE** UV-irradiated samples at different temperature between 100 and 180 °C. The evaluation of the integral area of the curves is collected in Figure 4b as a function of temperature. It is evident that the highest heat of curing was obtained at 160 °C, which was therefore settled as the temperature to achieve crosslinking reaction of the previous linear photoinduced formed polymer chains.

DSC analyses were also conducted to determine the T_g for the UV-irradiated polymer and for the network that underwent UV irradiation and thermal postprocess. The results provided a further validation of the occurring cross-linking reaction. The DSC scan related to the UV-irradiated polymer showed a T_g of about −25 °C and an exothermal peak with a maximum around 160 °C (see Figure S5 in the Supporting Information). The UV-irradiated **FGE** sample after the thermal treatment showed and enhancement of the T_g up to 52 °C and the absence of any exothermal peak (Figure S6, Supporting Information). This substantial T_g enhancement (+75 °C) can be attributed to the formation of the cross-links between the linear polymer chains, and the disappearance of the exothermic peak can be due to the complete curing process during heating.

The thermo-mechanical behavior of the two materials was studied by means of DMTA. The storage modulus and the tanδ curves for the UV-irradiated FGE sample and for the thermal post-treated sample are reported in **Figure 5**. The T_g is evaluated as the maximum of tanδ curve and it confirmed the trend of the T_g observed on DSC scans. The UV-irradiated FGE sample had a T_g of 5 °C while the post-thermal cured FGE sample achieved a

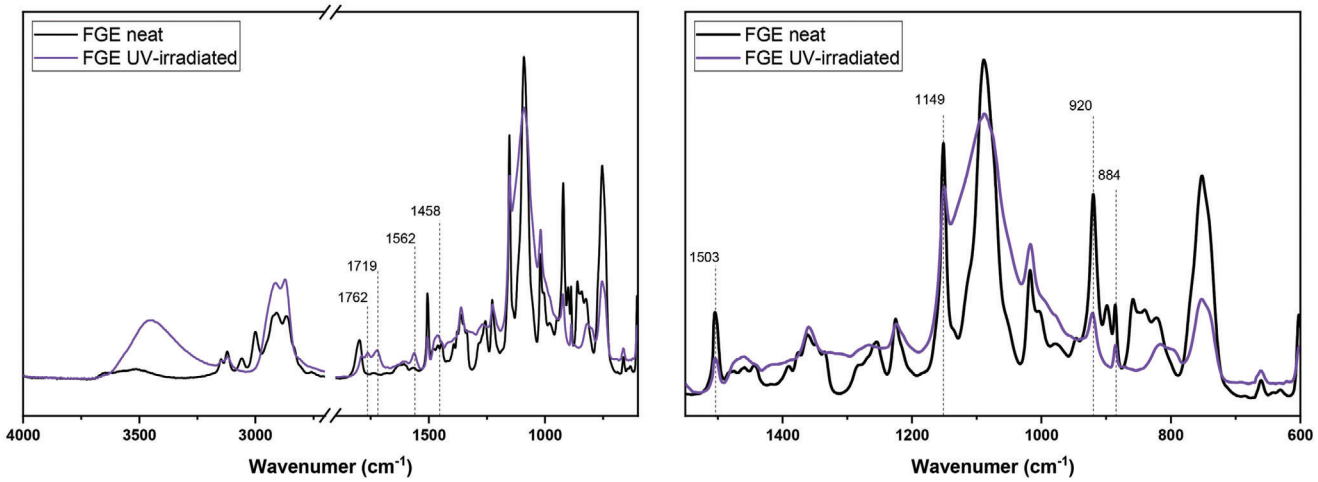

Figure 2. FTIR spectra of the FGE neat and UV-irradiated. As it can be notice the changes in the left spectra are highlighted in correspondence of 1762, 1719, 1562, and 1458 cm^{-1} considering the hypothesis of Mechanism 1. Instead, the right spectra show the decrease in the furan peaks at 1503, 1149, 920, and 884 cm^{-1}.

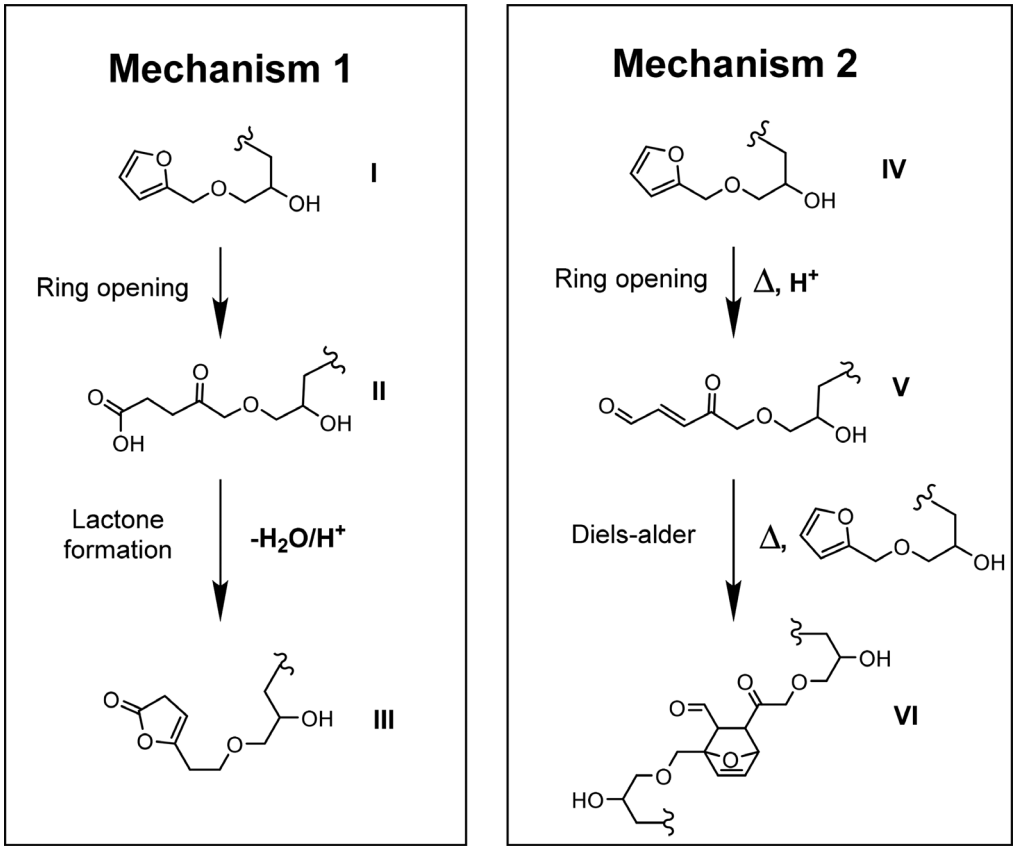

Scheme 2. Proposed reactions that could happen in the two-steps process based on FTIR investigations. Lactone formation (Mechanism 1) and Diels–Alder reaction (Mechanism 2).

T_g of 96 °C. The storage modulus of the two materials had an important change after the thermal treatment. As it can be noticed in Figure 5 the storage modulus showed an important increase when the polymer underwent thermal treatment. This can be explained by the formation of cross-links inside the network which contributes to increase the rigidity of the material. Indeed, the post-thermal treated FGE sample had a modulus of 2×10^{11} Pa in the rubbery region while the UV-irradiated FGE just reached the value of 8×10^{7} Pa.

The thermal crosslinking reaction also induced an enhancement of the thermal stability as demonstrated from TG analyses. As shown in Figure S7 (Supporting Information), the thermal

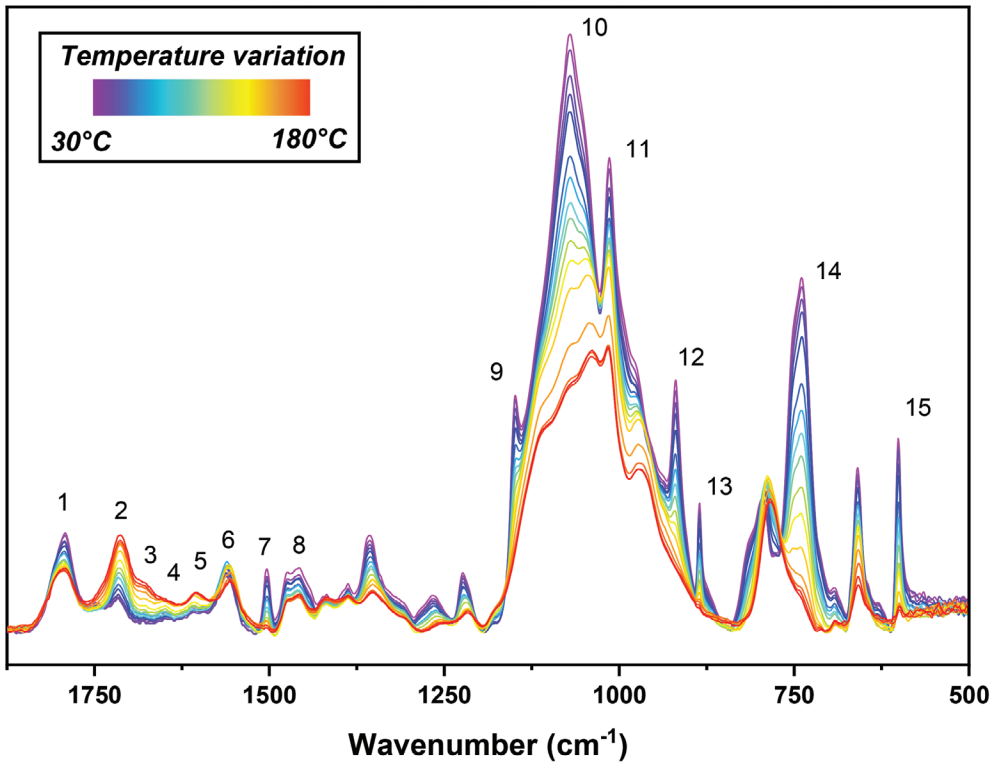

Figure 3. ART-FTIR spectra obtained in non-isothermal condition on UV-irradiated polymer. The temperature steps were 10 °C for each scan. The numbers (from **1** to **15**) highlight the characteristic peaks that change during the thermal treatment.

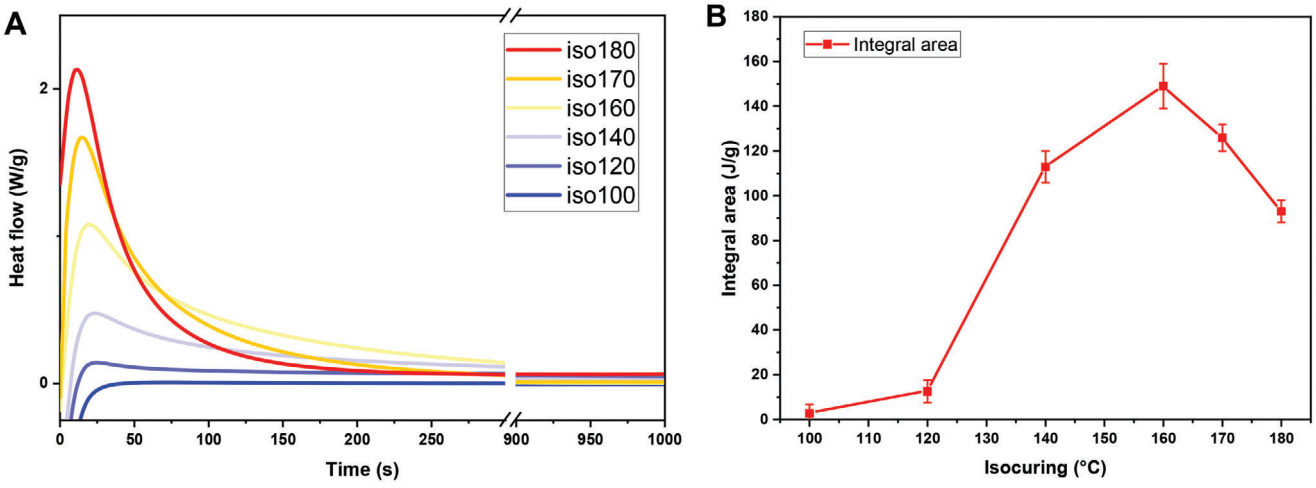

Figure 4. On the left A) the isothermal curing heat flow curves as a function of time of UV-irradiated FGE samples (100 °C / 120 °C / 140 °C / 160 °C / 170 °C / 180 °C). While on the right B) the result of the integration of the heat flow evaluated at each temperature.

stability changed for the two tested materials. Considering $T_{5\%}$, it can be noticed an increase of about 40 °C passing from 257 °C for the UV-irradiated material to 308 °C for the thermoset derived after thermal post-treatment.

The gel content evaluation is finally in accordance with the proposed mechanism since the UV-irradiated sample showed a gel content of 63%, while the thermal post-treatment was almost insoluble with a gel content of 98%.

3. Conclusion

This work demonstrates the possibility to achieve a cross-linked network starting from a monofunctional furan-based epoxy monomer under UV-irradiation and following thermal treatment. Furfuryl alcohol demonstrated to be a suitable biobased starting monomer to develop new epoxy thermosets. The exploitation of cationic UV induce polymerization leads

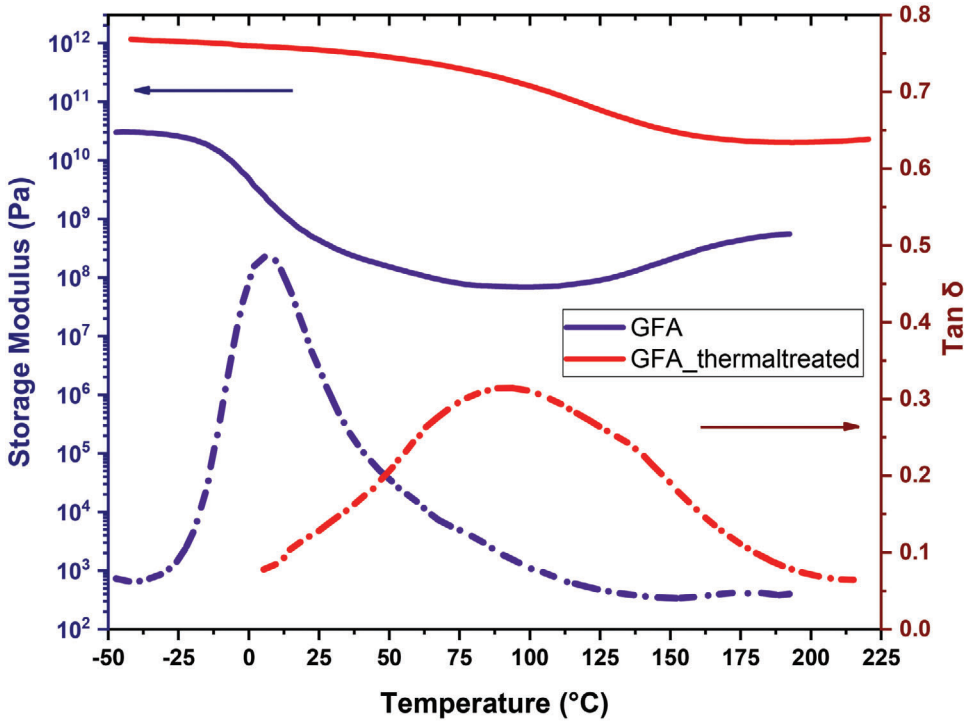

Figure 5. Tan δ and the Storage Modulus of the two tested materials measured by means of DMTA. The UV-irradiated FGE (purple line) and the post-thermal treated FGE (red line).

to formation of linear polymer chains generated from the ring-opening reaction of furfuryl glycidyl ether, FGE. Then, the thermal treatment of the achieved linear polymers gives the possibility to form cross-links between the polymer chains exploiting the reaction between the furan rings and an internally formed dienophile after ring opening (**V**). The occurring of the cross-linking reaction was confirmed with different analysis. The ATR-FTIR analysis qualitatively showed the change of the spectra during the thermal treatment. The evidence of the cross-links was corroborated by the appearance of new peaks in region between 1750 and 1550 cm^{-1} and the decrease of the peaks at 1503, 1149, 920, and 884 cm^{-1} distinctively associated to furan rings. From DSC analysis it was possible to understand the best curing condition to obtain the higher degree of crosslinking. After this primary study, the thermoset was characterized to compare the properties with the material obtained with only the UV-irradiation step. The investigation of the T_g by means of DMTA and DSC showed a substantial increase of T_g with respect to the UV-irradiated polymer. Moreover, the DMTA confirmed the increased elastic modulus associated with an increased rigidity after thermal curing attributed to the formation of additional cross-links between the polymer chains. As last validation of the entire cross-link step, the gel content of the thermal treated polymer showed a very high level of insoluble fractions due to the presence of cross-links between the polymeric chains.

4. Experimental Section

Materials: Furfuryl alcohol with purity of 98% (FA), epichlorohydrin (ECH) (purity > 99%), sodium hydroxide (NaOH), tetrabutylammonium hydrogen sulfate (TBHS), purity 97%, magnesium sulphate ($MgSO_4$) were purchased by Sigma Aldrich. Ethyl acetate, EtOAC, was supplied by Carlo Erba. NMR analysis was performed with deuterated chloroform, $CDCl_3$, provided by Sigma Aldrich. The photoinitiator, triarylsulfonium hexafluoroantimonate salts mixed to 50 wt% in propylene carbonate was purchased from Sigma Aldrich.

Monomer Synthesis: Epoxidation of Furfuryl Alcohol: Furfuryl glycidyl ether (FGE) was synthetized based on previous protocol reported in literature.[10,30] The etherification reaction is reported in **Scheme 3**.

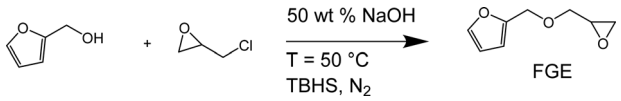

Scheme 3. Epoxidation of furfuryl alcohol.

Epichlorohydrin (28.3 g, 0.31 mol) was poured into a three round bottom flask; a solution of NaOH 50 wt % (11.2 g, 0.28 mol) was added. The TBHS (0.33 g, 0.001 mol) was used as transfer catalyst and added to the flask. The solution was stirred for 30 min at room temperature, and nitrogen atmosphere was provided to the system. Furfuryl alcohol (10.0 g, 0.10 mol) was slowly added, and the reaction time was 24 h during which the temperature was set at 50 °C. The reaction was stopped by adding ice water into the mixture. The product was extracted with ethyl acetate and dried over $MgSO_4$. Vacuum distillation was used to eliminate the solvent and the crude was left for 24 h in a vacuum oven (35 °C) to give yellowish liquid (12.2 g, yield 78%). The ^{1}H NMR and ^{13}C NMR spectra give the following signals

^{1}H NMR (400 MHz, CDCl3) δ 7.41 (t, J = 1.3 Hz, 1H), 6.34 (d, J = 1.6 Hz, 2H), 4.51 (m, 2H), 3.75 (dd, J = 11.5, 3.1 Hz, 1H), 3.44 (dd, J = 11.5, 5.8 Hz, 1H), 3.16 (ddt, J = 5.8, 4.2, 2.9 Hz, 1H), 2.79 (dd, J = 5.0, 4.1 Hz, 1H), 2.61 (dd, J = 5.0, 2.7 Hz, 1H).

^{13}C NMR (101 MHz, CDCl3) δ 151.51, 143.08, 110.43, 109.73, 70.72, 65.20, 50.87, 44.46.

Photopolymerization and Thermal Crosslinking: The monofunctional monomer **FGE** (usually around 0.4 g) was poured into a vial and then the photoinitiator was added as 2 per hundred resin (phr). The formulation was mixed mechanically for 5 min and the vial was wrapped with aluminum foil to avoid light contact. The formulations were spread on glass substrate with a film bar ensuring a thickness of 150 µm. The irradiation step was carried out by exposing the formulation to UV-light for 2 min. DMAX Flood lamp was used as UV-light source with light intensity set around 130 mW cm^{-2}. After the thermal treatment on the photocured films was done in an oven at 160 °C for 1 h.

Characterization: NMR—NMR was conducted on a Bruker AM 400. ^{1}H-NMR and ^{13}C-NMR spectra were recorded at 400 and 101 MHz respectively. $CDCl_3$ was used as solvent.

FTIR—The epoxy ring open was followed by means of real-time FTIR analysis. The samples were analyzed by means of a Perkin Elmer Spectrum 2000 FTIR spectrometer in transmittance mode. The liquid formulations were spread on silicon wafer with a thickness of 12 µm by means of film bar. The intensity of the UV light was set as 130 mW cm^{-2}. The evaluation of the conversion was done according to the decrease of epoxy peak situated at 860 cm^{-1}. All data were recorded as 32 scans with a spectral resolution of 4.0 cm^{-1} and handled with the software Omnic from Thermo Fischer Scientific.

Some FTIR analyses were also done on the thermal treated samples and in non-isothermal condition. In this case, a Thermo Fischer IS-20 spectrometer in equipped with a hot-plate GladiATR device (Pike Technologies) with a monolithic diamond ATR configuration. The spectra were collected from 30 to 180 °C (each step was 10 °C). The spectrum of air was recorded as background. A total of 64 scans with a resolution of 4 cm^{-1} were recorded for each sample. The data were handle with the software Omnic from Thermo Fischer Scientific.

Electrospray-Mass Spectrometry (ESI/MS)—The molecular weight of the linear polymer chains was evaluated by means of mass spectrometry. The irradiated samples were dissolved in $CHCl_3$ and then they were solubilized in acetonitrile, the solvent used for the test. The solution was introduced into a classic (LCQ) quadrupole ion trap (Thermo Scientific, San Jose, CA, USA) equipped with an electrospray source. The spectra were acquired in the range m/z 200–800 in the positive mode. The electrospray source and ion trap were operated under the following conditions: flow rate, 5 µL min^{-1}, electrospray ionization voltage, 4.5–5 kV. The ESI-MS technique uses a soft ionization process that does not fragment compounds and provides molecular weight information with unit mass resolution.

Gel Count—The gel content percentage (% gel) of the polymers was determined by measuring the weight loss after 24 h extraction with chloroform. The samples after the immersion were allowed to dry for 24 h in air. % gel was calculated according to Equation (1)

$$\%\ \text{gel} = \frac{W_1}{W_0} \times 100 \quad (1)$$

where W_1 is the weight of the dry film after the treatment with chloroform and W_0 is the weight of the dry sample before the treatment.

DMTA—The thermal mechanical analysis of the polymers was carried out with a Triton Technology instrument. The instrument applied uniaxial tensile stress at frequency of 1 Hz with a heating rate of 3 °C min^{-1}. The initial temperature of −40 °C was achieved by cooling down the test chamber with liquid nitrogen. The measurements were done to detect the T_g as maximum of tanδ curve and were stopped after the rubbery plateau. The samples had dimension of 12 mm x 4 mm x 0.3 mm and they were UV-irradiated in a silicon mold.

Thermogravimetric Analysis (TGA)—The thermal stability of the polymers was studied by means of a Mettler Toledo TGA1. The test was done imposing a heating ramp of 10 °C min^{-1} from room temperature to 700 °C under N_2 atmosphere with flow of 40 mL min^{-1}. The analysis was done considering different features: $T_{5\%}$, temperature at which the sample lost 5 wt%; T_{peak}, temperature at peak of degradation, evaluated as peak of the first derivative and final char residue, analyzed as wt%.

DSC—The DSC analysis was performed on a Mettler Toledo DSC-1 equipped with Gas Controller GC100. The data were analyzed with Mettler Toledo STARe software V9.2. Samples of about 5–10 mg were sealed in 40 µL aluminum pans and analyzed by DSC.

The thermal curing step was studied by means of DSC analysis on UV-irradiated samples. An isocuring stage was performed to evaluate the heat released during the curing. The characteristics of the tests were the following: 1 h at different temperatures, 100, 120, 140, 160, 170, and 180 °C.

The UV-irradiated and the UV-irradiated + thermal treated samples were also studied with DSC. The samples were analyzed applying the following method: the first dynamic stage was set from room temperature to −60 °C, then 5 min of stabilization were set; the first heating was then performed from −60 to 240 °C; then the temperature was decreased again to −60 °C and a final heating step was performed until 300 °C. The heating and the cooling rates were the same for all dynamic stage and were set at 10 °C min^{-1}. The analysis was performed in a nitrogen atmosphere with a flow rate of 40 mL min^{-1}.

Supporting Information

Supporting Information is available from the Wiley Online Library or from the author.

Acknowledgements

Open Access Funding provided by Politecnico di Torino within the CRUI-CARE Agreement.

Conflict of Interest

The authors declare no conflict of interest.

Data Availability Statement

The data that support the findings of this study are available from the corresponding author upon reasonable request.

Keywords

cationic UV-cures, cross-links, epoxies, furans, monofunctional monomers

Received: January 10, 2022
Revised: March 1, 2022
Published online:

[1] A. Gandini, T. M. Lacerda, A. J. F. Carvalho, E. Trovatti, *Chem. Rev.* **2016**, *116*, 1637.
[2] B. M. Upton, A. M. Kasko, *Chem. Rev.* **2016**, *116*, 2275.
[3] A. F. Sousa, C. Vilela, A. C. Fonseca, M. Matos, C. S. R. Freire, G.-J. M. Gruter, J. F. J. Coelho, A. J. D. Silvestre, *Polym. Chem.* **2015**, *6*, 5961.
[4] A. Gandini, T. M. Lacerda, *Prog. Polym. Sci.* **2015**, *48*, 1.
[5] A. Corma, S. Iborra, A. Velty, *Chem. Rev.* **2007**, *107*, 2411.
[6] D. K. Mishra, S. Kumar, R. S. Shukla, *Biomass, Biofuels, Biochem*. **2020**, https://doi.org/10.1016/B978-0-444-64307-0.00012-3.
[7] E. M. Lems, S. Winklehner, C. Hansmann, W. Gindl-Altmutter, S. Veigel, *Cellulose* **2019**, *6*.

[8] R. Marefat Seyedlar, M. Imani, S. M. Mirabedini, *Polym. Bull.* **2021**, *78*, 577.
[9] S. Dello Iacono, A. Martone, E. Amendola, *Paint Coatings Ind.* **2019**, https://doi.org/10.5772/intechopen.81360.
[10] L. Pezzana, G. Melilli, N. Guigo, N. Sbirrazzuoli, M. Sangermano, *ACS Sustainable Chem. Eng.* **2021**, *9*, 17403.
[11] R. Mariscal, P. Maireles-Torres, M. Ojeda, I. Sádaba, M. López Granados, *Energy Environ. Sci.* **2016**, *9*, 1144.
[12] K. J. Zeitsch, *The Chemistry Nad Technology of Furfural and its Many by-Products*, Elsevier, Amsterdam, the Netherlands, **2000**.
[13] M. Choura, N. M. Belgacem, A. Gandini, *Macromolecules* **1996**, *29*, 3839.
[14] G. Tondi, N. Cefarin, T. Sepperer, F. D'amico, R. J. F. Berger, M. Musso, G. Birarda, A. Reyer, T. Schnabel, L. Vaccari, *Polymers (Basel)* **2019**, *11*, 2126.
[15] N. Guigo, A. Mija, L. Vincent, N. Sbirrazzuoli, *Phys. Chem. Chem. Phys.* **2007**, *9*, 5359.
[16] M. Sangermano, N. Razza, J. V. Crivello, *Macromol. Mater. Eng.* **2014**, *299*, 775.
[17] C. Decker, *Macromol. Rapid Commun.* **2002**, *23*, 1067.
[18] M. D. Purbrick, *Polym. Int.* **1996**, *40*, 74.
[19] A. B. Scranton, C. N. Bowman R. W. Peiffer, *Photopolymerization: Fundamentals and Applications*, ACS symposium series, American Chemical Society, USA **1997**.
[20] Y. Yagci, *Macromol. Symp.* **2006**, *240*, 93.
[21] J. V. Crivello, J. H. W. Lam, *Macromolecules* **1977**, *10*, 1307.
[22] J. V. Crivello, J. H. W. Lam, *J. Polym. Sci., Polym. Chem. Ed.* **1979**, *17*, 2877.
[23] L. Pezzana, E. Malmström, M. Johansson, M. Sangermano, *Polymer* **2021**, *13*.
[24] C. Noè, M. Hakkarainen, M. Sangermano, *Polymers (Basel)* **2021**, *13*, 1.
[25] J. V. Crivello, R. Narayan, *Chem. Mater.* **1992**, *4*, 692.
[26] S. Malburet, C. D. Mauro, C. Noé, A. Mija, M. Sangermano, A. Graillot, *RSC Adv.* **2020**, *10*, 41954.
[27] C. Noè, S. Malburet, E. Milani, A. Bouvet-Marchand, A. Graillot, M. Sangermano, *Polym. Int.* **2020**, *69*, 668.
[28] C. Noè, L. Iannucci, S. Malburet, A. Graillot, M. Sangermano, S. Grassini, *Macromol. Mater. Eng.* **2021**, *306*, 2100029.
[29] S. Nameer, D. B. Larsen, J. Ø. Duus, A. E. Daugaard, M. Johansson, *ACS Sustainable Chem. Eng.* **2018**, *6*, 9442.
[30] J. K. Cho, J.-S. Lee, J. Jeong, B. Kim, B. Kim, S. Kim, S. Shin, H.-J. Kim, S.-H. Lee, *J. Adhes. Sci. Technol.* **2013**, *27*, 2127.
[31] S. Brännström, M. Johansson, E. Malmström, *Biomacromolecules* **2019**, *20*, 1308.
[32] G. Falco, N. Guigo, L. Vincent, N. Sbirrazzuoli, *ChemSusChem* **2018**, *11*, 1805.
[33] R. Zhu, A. Chatzidimitriou, B. Liu, D. J. Kerwood, J. Q. Bond, *ACS Catal.* **2020**, *10*, 1555.
[34] S. Dutta, I. K. M. Yu, D. C. W. Tsang, Y. H. Ng, Y. S. Ok, J. Sherwood, J. H. Clark, *Chem. Eng. J.* **2019**, *372*, 992.
[35] F. D'amico, M. E. Musso, R. J. F. Berger, N. Cefarin, G. Birarda, G. Tondi, D. Bertoldo Menezes, A. Reyer, L. Scarabattoli, T. Sepperer, T. Schnabel, L. Vaccari, *Spectrochim. Acta, Part A* **2021**, *262*, 120090.
[36] A. Dell'acqua, B. M. Stadler, S. Kirchhecker, S. Tin, J. G. De Vries, *Green Chem.* **2020**, *22*, 5267.